

Article

A Correlation Relating the Residual Strength Parameters to the Proportions of Clay Fractions and Plasticity Characteristics of Overburden Sediments from the Open-Pit Mine Drmno

Stevan Ćorluka ^{1,*}, Dragoslav Rakić ², Nikola Živanović ³, Ksenija Djoković ¹ and Tina Đurić ²¹ Institute for Materials Testing—IMS, 11040 Belgrade, Serbia; ksenija.djokovic@institutims.rs² Faculty of Mining and Geology, The University of Belgrade, 11000 Belgrade, Serbia; dragoslav.rakic@rgf.bg.ac.rs (D.R.); tina.djuric@rgf.bg.ac.rs (T.Đ.)³ Faculty of Forestry, The University of Belgrade, 11030 Belgrade, Serbia; nikola.zivanovic@sfb.bg.ac.rs

* Correspondence: stevan.corluka@institutims.rs

Abstract: One of the prerequisites for the safe exploitation of surface mines is the stability of the working and final slopes of the mine. In order to ensure this, it is necessary to carry out detailed field and laboratory geomechanical tests of the soil and, based on the obtained results, make calculations related to stability analyses. The results obtained in this way are used for dimensioning the slope of exploitation slopes (excavation). Landslides occur when the ultimate shear strength is reached, and therefore, the adequate definition of shear strength parameters is one of the essential prerequisites for successfully solving the stability problem. Unlike earlier tests in Serbia, when the residual shear strength parameters were determined based on the usual conventional methods (direct shear apparatus, triaxial apparatus), this time, in addition to the direct shear apparatus, a ring shear apparatus was also chosen for testing. The paper shows the method of determining the residual shear strength parameters of high plasticity gray clays and siltstones of roof sediments from open pit mine Drmno, using direct and ring shear apparatus. The results show that the residual angle of internal friction for gray clays obtained with the ring shear apparatus is 9.9–10.8°, and for the siltstone, it is 11.8–12.9°, both of which are lower than the values obtained with the direct shear apparatus. In addition, correlations between the residual parameters of soil shear resistance and some physical indicators (plasticity index, clay content) are provided, showing high correlation coefficients. The proposed correlations should be used only when time and financial constraints prevent the execution of actual tests to determine residual shear strength, as concrete experimental procedures provide a much more reliable assessment of the residual strength properties of the soil.

Keywords: residual strength of soil; ring shear apparatus; direct shear apparatus; slope stability; open pit mines



Citation: Ćorluka, S.; Rakić, D.; Živanović, N.; Djoković, K.; Đurić, T. A Correlation Relating the Residual Strength Parameters to the Proportions of Clay Fractions and Plasticity Characteristics of Overburden Sediments from the Open-Pit Mine Drmno. *Appl. Sci.* **2024**, *14*, 10325. <https://doi.org/10.3390/app142210325>

Academic Editor: Yosoon Choi

Received: 19 September 2024

Revised: 31 October 2024

Accepted: 3 November 2024

Published: 10 November 2024



Copyright: © 2024 by the authors. Licensee MDPI, Basel, Switzerland. This article is an open access article distributed under the terms and conditions of the Creative Commons Attribution (CC BY) license (<https://creativecommons.org/licenses/by/4.0/>).

1. Introduction

In the analysis of slopes that have experienced large shear displacements, the relevant factor is the residual shear strength of the soil. This is most commonly determined based on laboratory tests using a direct shear apparatus by performing a reverse test, or using an apparatus that allows unlimited horizontal deformation (ring shear apparatus). In geotechnical practice in Serbia, as well as globally, the use of the ring shear apparatus is not common, given that it falls under research equipment rather than standard laboratory equipment.

The direct shear test is the oldest and simplest type of laboratory testing for shear strength. This conceptually simple test has been used to assess soil since 1776 by Coulomb [1], and it was notably highlighted by French engineer Alexandre Collin in 1846 [2]. In Britain, Bell (1915) recorded the first measurements and constructed a device intended to be a prototype for the later development of the direct shear apparatus. Bell was the first to

conduct and publish practical results of shear strength testing for different soil types [3,4]. The modern shear box was designed by Casagrande at Harvard University (USA) in 1932 [5]. An apparatus with a constant deformation rate applying the “controlled deformation” principle using a fixed-speed motor was developed in 1946 [6], Bishop, 1946 presented detailed design improvements using this principle. Vickers, 1984 developed another shear apparatus capable of performing both drained and undrained tests [7].

Today, there are many devices from different manufacturers used for conducting direct shear tests, which fundamentally do not differ much in their testing mechanisms.

It was in 1936 and 1939 that Hvorslev proposed the first general concept for constructing a ring shear apparatus [8,9]. Following this, several different designs of the apparatus were developed based on this concept; examples include: La Gata (1970), Bishop et al. (1971), Bromhead (1979), Savage and Sayed (1984), Hungr and Morgenstern (1984), Tika (1989), and Garga and Sendano (2002) [10–16]. However, the ring shear apparatus constructed by Bromhead in 1979 has become increasingly popular due to its affordability and ease of use [12]. Bromhead and Curtis (1983) demonstrated that this apparatus produces results consistent with those obtained using more sophisticated devices developed by the Norwegian Geotechnical Institute and Imperial College [17]. Since 1984, Prof. Sassa et al. from the Disaster Prevention Research Institute (DPRI) at Kyoto University have developed seven designs of ring shear apparatuses that allow for the laboratory simulation of seismic impacts and the measurement of pore pressures during undrained tests through a control system [18].

The concept of residual shear strength first appeared in the literature in 1937 [19]. The residual shear strength of soil is an important parameter in geotechnical engineering. It is the strength reached after large displacements. Further shearing in the same direction does not lead to a decrease in shear strength, as it remains constant; thus, there are no further changes in volume or changes in excess pore pressures.

Understanding residual shear strength at large displacements is crucial in explaining the mechanism of sliding [2,16,20]. Conventional laboratory methods for defining shear strength, such as the direct shear test, allow for maximum displacements up to 10 mm for samples measuring 6×6 cm [21–23]. For these reasons, assessing soil behavior at large displacements is challenging since residual shear strength can only be defined through multiple shear cycles. The ring shear test, which allows unlimited displacement of the sample, is a much more reliable method for determining residual shear strength [22,24], as evidenced by several scientific studies [25–28]. For example, Fukuoka et al. (2007) applied a new concept using the ring shear test to define shear zones that occur at large displacements. This study indicated that the ring shear test is most suitable for studying landslides, where large displacements typically occur [26]. Kimura et al. (2014) investigated the effect of shear rate in defining the residual shear strength of soil in a landslide using the ring shear test [29]. In the new Eurocode 7: Part 2: 2007 regulations, it is stated that, during tests to determine soil residual strength parameters, it is necessary to ensure the parallel alignment of boxes during shearing, which can only be achieved with a ring shear apparatus [30]. However, it should be noted that, in geotechnical practice, results from reverse direct shear tests are still most commonly used to define residual shear strength parameters. Significant displacements are required to accurately define residual shear strength, and these can only be approximately reproduced in the ring shear apparatus.

This paper presents the results of testing the residual shear strength parameters of soil using a direct shear apparatus (DS) and a ring shear apparatus (RS). The primary goal is to determine the difference in values obtained using these two different apparatuses. The secondary aim is to establish the correlation of residual shear strength parameters with certain physical indicators, as well as the relationship between residual parameters and normal stresses.

2. Materials and Methods

The Drmno deposit is part of the Kostolac coal basin and is located on the right bank of the Danube, approximately 90 km downstream from Belgrade. The deposit encompasses the area east of the Mlava River, and its boundaries are defined by: the Danube River to the north, Boževačka Greda to the east, the Bradarac-Sirovačka Valley line to the south, and the Mlava River to the west (Figure 1a,b).

2.1. The Broader Geological Structure of Open Pit Mine Drmno

The broader area of Kostolac is composed of formations from the Paleozoic, Neogene, and Quaternary periods.

The Drmno deposit consists of three coal layers designated as III, II, and I (from the oldest to the youngest, respectively). The third (III) coal layer is the deepest and oldest. The second (II) coal seam occurs above the third layer and extends northwest of open pit mine "Drmno," near the Kostolac B Power Plant. In the far northwest part of the deposit, the first (I) coal layer extends, covering a small area (Figure 1c).

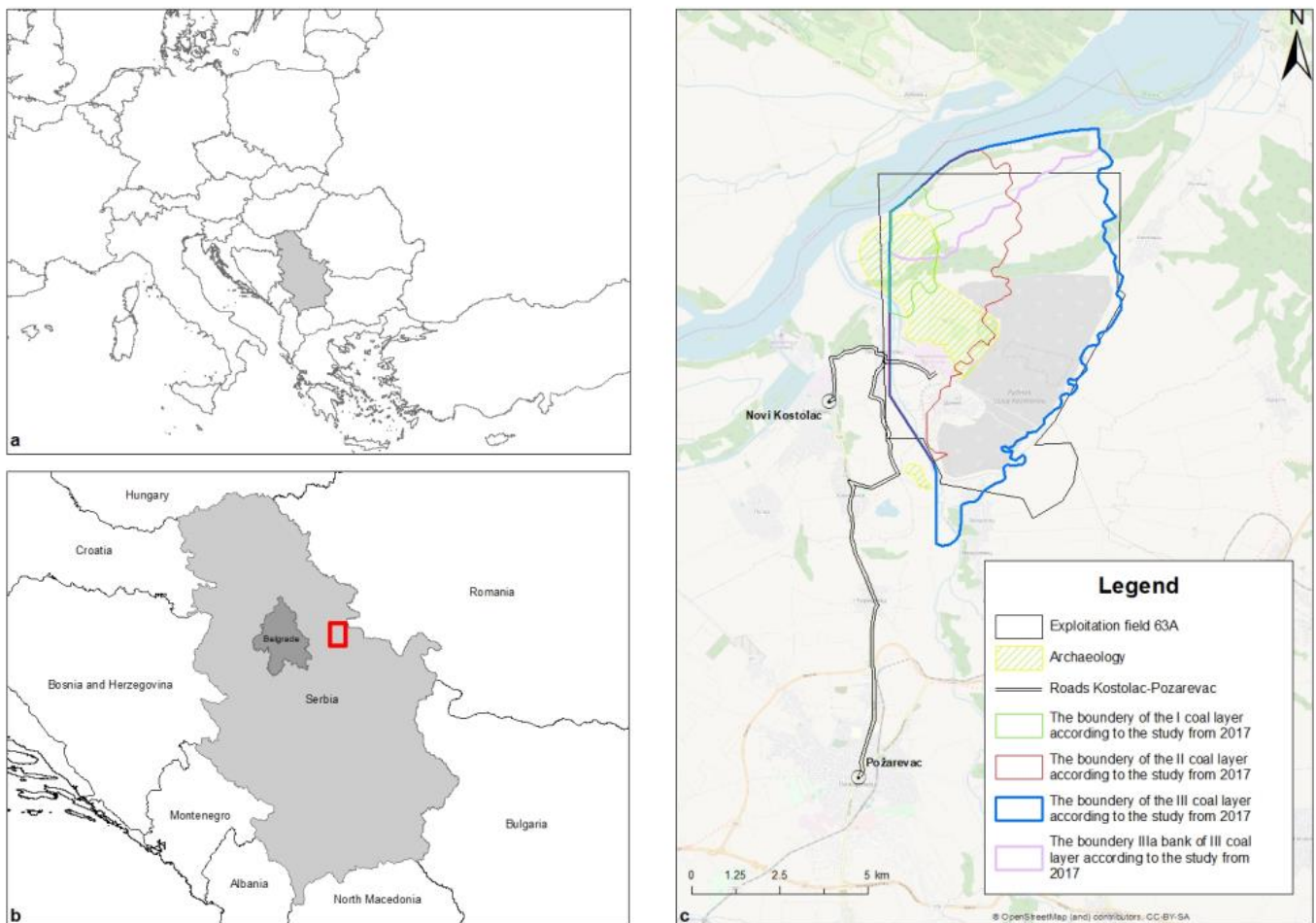


Figure 1. (a). Position of Serbia in relation to Europe. (b). Position of the Kostolac area in relation to Serbia. (c). Position of the Drmno deposit in relation to Kostolac.

The third coal layer is deposited over clayey–sandy sediments of the lower Pontian. In the Drmno deposit area, it is continuous across almost the entire expanse, occasionally with interlayers of carbonaceous clay, silt, and sand.

The thickness and number of overburden layers vary. The highest number of overburden layers occurs in the western part of the deposit. The overburden interlayers identified in the third coal layer are mostly composed of siltstone. Sandy sediments appear less frequently, primarily in the northern part of the deposit. Clay, as the overburden material, is found in the southern and central parts of the third coal layer. In the lowest parts of the third layer, interlayers composed of siltstone and carbonaceous clay occur.

The first coal layer is defined in the far northwest part of the deposit and is parallel to the second and third coal seams.

The overburden deposits can be divided into direct overburden, interburden, and floor.

Direct overburden—Quaternary formations are represented by gravel, sand, occasionally clay, and loess.

Interburden—The overlying material of the third coal layer is composed of sand with interlayers of carbonaceous, sandy, and marl clay, siltstone, and coal.

The floor of the second coal layer is composed of sand, carbonaceous clay, clayey silt, and siltstone. The overlying material of the second coal layer, where it is developed, consists of sand, clayey sand, carbonaceous clay, marl clay, siltstone, and rare coal interlayers. The youngest upper Pontian sediments are composed of gray-blue clay, sand, and clayey sand with interlayers of carbonaceous clay and coal.

Floor—In the immediate floor of the third coal layer, there are deposits of sand and clay that are gray and black in color (when containing organic matter), and within these layers, individual lenses and interlayers of coal appear (Figure 2).

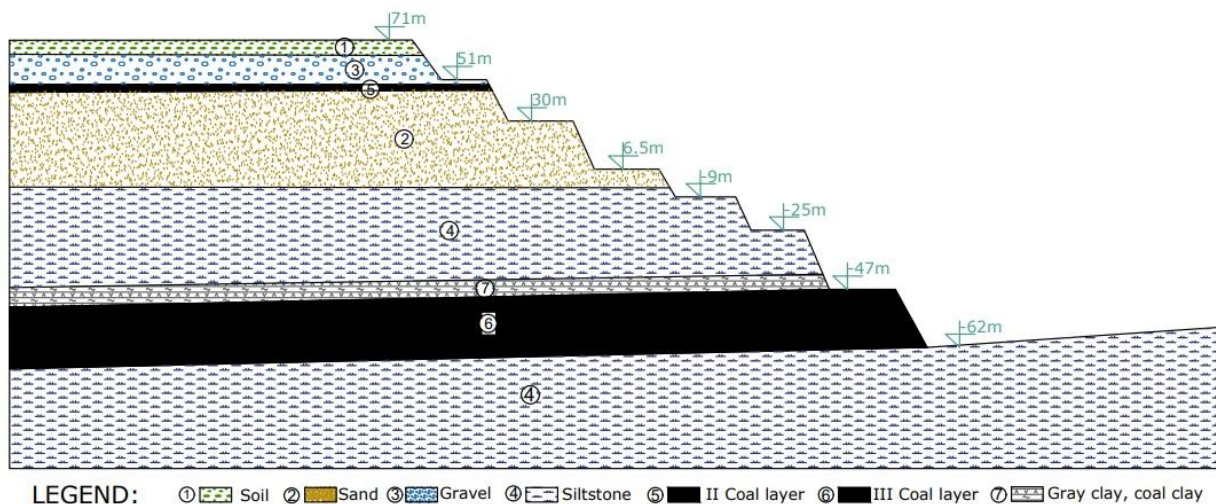


Figure 2. Schematic representation of the final western slope of the open pit mine: 1: humus; 2: sand; 3: gravel; 4: siltstone; 5: second coal layer; 6: third coal layer; 7: gray clay.

2.2. Samples for Testing

Local instabilities due to exploitation on working slopes appear as step-like slides in the overlying silty and clayey materials, as these are the most sensitive to changes in moisture and external influences. Historically, the monitoring of the surface mine has recorded over a hundred parallel tension cracks on the surface, which occur with shallow landslides. Their sliding bodies are shallow and do not exert significant pressure on the stable part of the terrain, thus not causing an increase in pore pressures along the slip plane. Ground sliding is the result of the action of groundwater along the tension cracks. This water can be wandering, capillary, or originate from higher layers of gravel and coarser sands. Intense rainfall increases the volume of groundwater in the soil, which, under the influence of gravity, machine vibrations, and pressure from layers above, moves to lower elevations, forming unstable blocks of silty-clayey materials.

Due to the frequent occurrence of local sliding on working slopes above the third coal layer, laboratory tests were conducted on overburden sediments for this study using a total

of 6 samples. These included siltstones from layer no. 4 (3 samples: U-4, U-5, U-6) and gray clay from layer no. 7 (3 samples: U-7, U-8, U-9) (Figure 2).

2.3. Identification and Classification Testing

The identification and classification tests were conducted at the Geomechanics Laboratory of the Mining Institute in Belgrade. All tests were performed in accordance with the SRPS EN ISO 17892 standard [31–33].

2.4. Apparatus for Determining Residual Shear Strength

For the purposes of this research, tests of residual shear strength were conducted on selected soil samples using two apparatuses: the ring shear apparatus (RS) and the direct shear apparatus (DS).

The RS used in the research is based on the original design developed by Bromhead, 1979 [12] and is manufactured by Wykeham-Farrance Engineering Limited (Figure 3). The sample is ring-shaped with an internal diameter of 70 mm, an external diameter of 100 mm, and a height of 5 mm. The drainage of the sample is facilitated by two bronze porous discs attached to the bottom of the lower part and the top of the shear box.

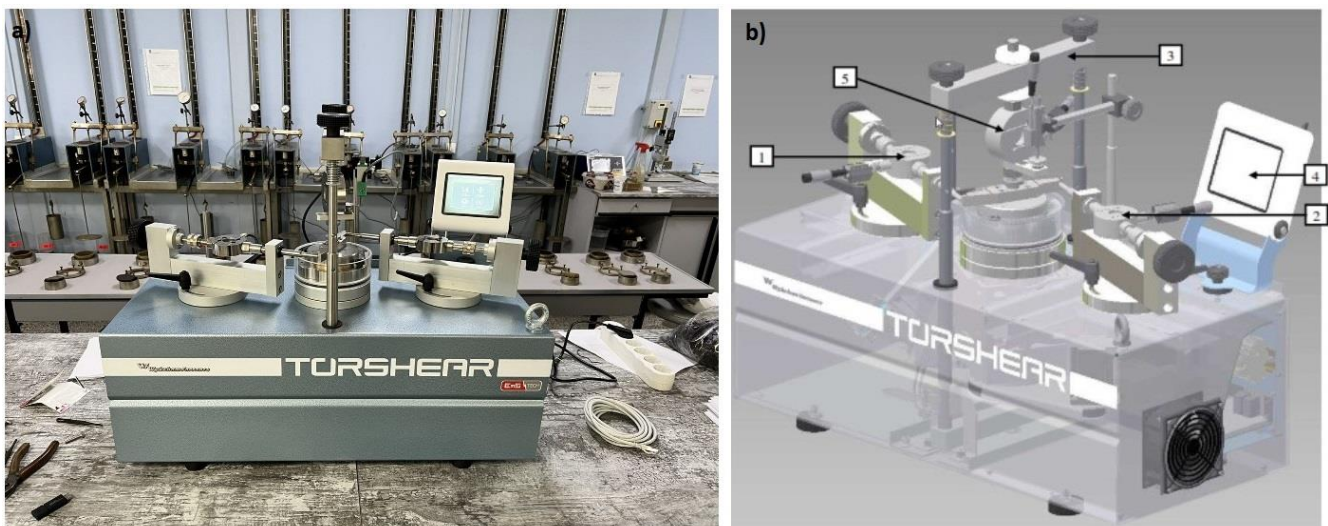


Figure 3. (a) Bromhead's ring shear apparatus. (b) Three-dimensional model of the ring shear apparatus (Source: manufacturer's manual). Legend: 1, 2—horizontal force measurement cell, 3—frame for transmitting vertical load, 4—touchscreen display, 5—vertical force measurement cell.

In the ring shear apparatus, during testing, the cross-sectional area of the sample remains constant, and thus, shear stresses are induced by torque.

The formula used to calculate residual shear strength is:

$$\tau_R = \frac{3(F_1 + F_2)L}{4\pi(R_2^3 - R_1^3)}, \quad (1)$$

where

τ_R —residual shear strength, kPa;

F_1, F_2 —force measured at the ends of the beam for transmitting torque, N;

R_1, R_2 —internal and external diameters of the sample, mm, respectively;

L —length of the torque beam, mm.

For determining the residual shear strength parameters using the direct shear test in a shear box, an apparatus manufactured by Matest in Italy was used (Figure 4). The sample was square-shaped with the dimensions of 60 × 60 mm, and the initial height of the sample was 21 mm.

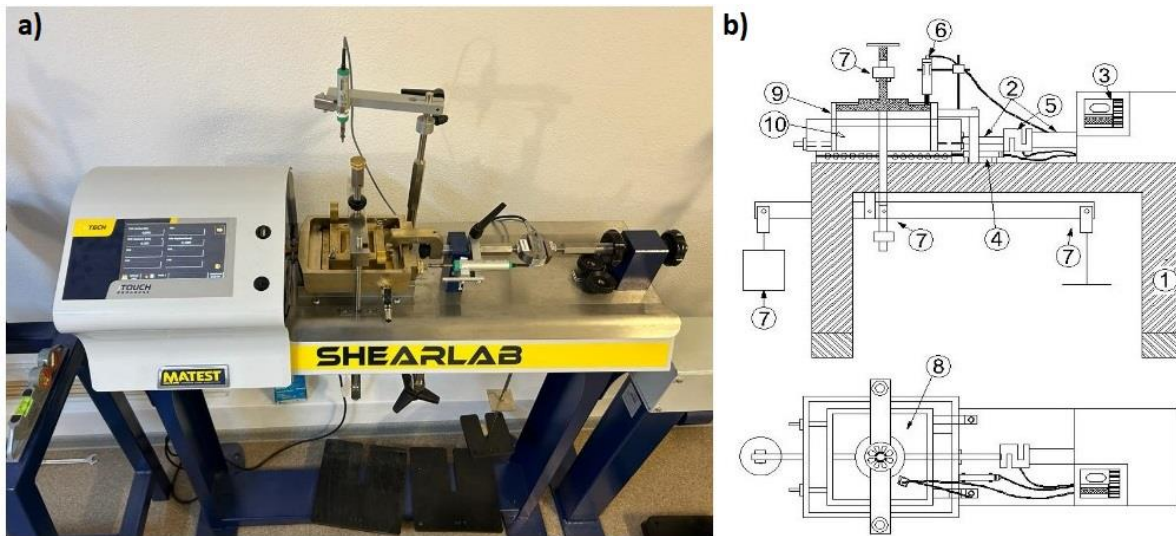


Figure 4. (a) Matest direct shear apparatus. (b) Two-dimensional model of the direct shear apparatus [34] (Reprinted/adapted with permission from Ref. [Karimpour F. et al., 2015]) Legend: 1—frame of the apparatus, 2—system for transmitting horizontal load, 3—digital control unit, 4—device for measuring horizontal linear displacements, 5—device for measuring horizontal load, 6—device for measuring vertical linear displacements, 7—system for transmitting vertical load, 8—plate for transmitting uniform vertical load, 9, 10—shear box.

The formula used to calculate residual shear strength in the direct shear test is:

$$\tau_R = \frac{P}{A} \quad (2)$$

where

τ_R —residual shear strength, kPa;

P —horizontal shear force, N;

A —the cross-sectional area of a sample, mm.

2.5. Testing Procedure

Remolded or reconstructed samples can be used to determine residual strength with DS and RS devices [2]. Bishop et al., 1971 [11] pointed out that the residual shear strength is not affected by the deformation of the samples (previous stress history). Remolded samples for testing were prepared first by air drying and then by grinding the soil in an avan. The samples were then sieved through a 1.0 mm sieve, mixed with distilled water to the desired moisture content for compaction, and allowed to hydrate for at least 24 h.

The remolded samples for testing were compacted directly into an oedometer apparatus with an outer diameter of 100 mm and incrementally loaded vertically up to a maximum vertical stress of 400 kPa. After 24 h, the sample was extruded from the oedometer mold and placed into the RS apparatus. For the DS apparatus, the samples were prepared in the same way as for the RS apparatus. Afterward, the sample was first compacted into a square mold with dimensions of 6 × 6 cm and then extruded into the shear box.

According to the recommendations of the ASTM D6467-13 standard [35], sample preparation at the liquid limit is advised for these tests. However, samples prepared at the liquid limit were not suitable for testing due to the extrusion of the sample around the porous stone during consolidation. Similar observations were noted by Hayden et al. (2018) and Kiernan et al., 2022 [36,37]. For this study, the samples were prepared with the moisture content close to the plastic limit. Figure 5 shows the appearance of the samples after testing in the ring shear and direct shear apparatuses.



Figure 5. Appearance of the gray clay samples after testing in the ring shear apparatus (left) and direct shear apparatus (right).

The samples were consolidated and sheared under vertical loads of 50, 100, 200, and 400 kPa. During shearing, a constant vertical pressure was maintained. In selecting the shear rate, the criterion was set to ensure the rate was slow enough to eliminate the occurrence of excess pore pressure on the failure plane at a predefined failure criterion. Ramiah et al., 1970 [38] found that the measured residual shear strength was not affected by an increase in displacement rate from 0.02 to 60 mm/min. Skempton, 1985 [12] concluded that there is less than 5% variation in the value of the angle of internal friction for shear rates ranging from 0.05 to 0.35 mm/min. The Japanese Geotechnical Society, 2010 [39] suggests a shear rate of 0.02 mm/min for direct shear apparatuses. To arrive at an acceptable shear rate for this study, remolded samples were tested at a shear rate of 0.02 mm/min in both apparatuses.

In an ideal scenario, the residual shear strength of soil can be defined as the shear strength at which shear stresses and the sample's volume remain constant with further increases in horizontal displacements (deformation) [40]. For the ring shear test, Bromhead, 1992 [41] concluded that, if the shear torque remains constant for more than 1 h, it indicates residual shear strength. In this study, the test samples were sheared to a displacement of about 360 mm, resulting in a constant torque value for at least the last 150 h of shearing.

2.6. Statistical Analyses

In the data analysis, descriptive statistics were used, including the determination of maximum, minimum, mean, and median values, as well as measures of sample variation (standard deviation and coefficient of variation). The Tukey–Kramer test was used to determine significant statistical differences. The significance of the relationship between variables was assessed using linear regression analysis. All analyses were conducted in EXCEL (MS Office 2010 Professional Plus, No. of ref: 977001862).

3. Results and Discussion

This study presents an analysis of results related to the residual shear strength obtained from highly plastic clayey and silty samples, which are part of the overburden of the third coal layer (Figure 2).

The analysis of the grain size distribution shows that the siltstone consists of 13–15% clay fraction, 81% silt fraction, and 4–6% sand fraction, while the gray clay layer consists of 30–34% clay fraction, 65–69% silt fraction, and 0–2% sand fraction. The results of these tests are presented in Figure 6.

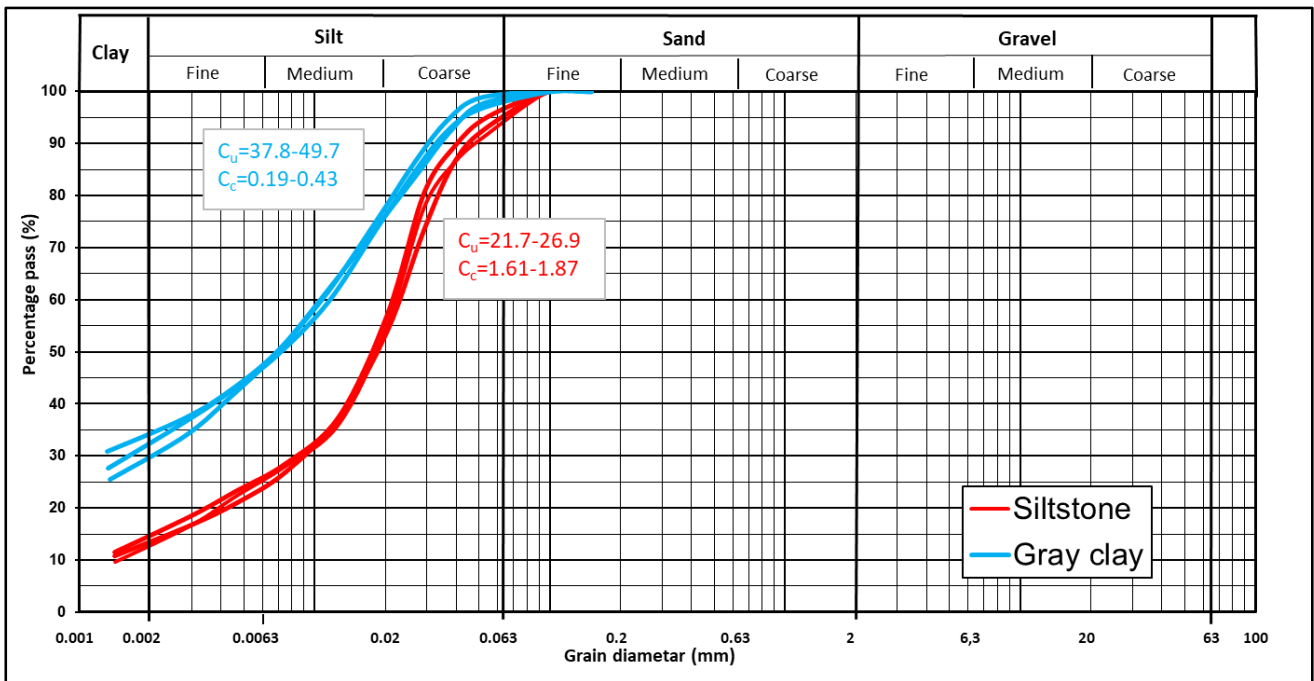


Figure 6. Particle size distribution graph.

The liquid limit is in the range of $LL = 46.3\text{--}47.5\%$ for siltstone and $LL = 63.0\text{--}68.0\%$ for gray clay samples. The plasticity index values are in the range of $I_p = 19.7\text{--}21.6\%$ for siltstone and $I_p = 22.5\text{--}23.2\%$ for gray clay. According to the plasticity chart in EN ISO 14688-2 (2018) [42], based on the liquid limit and plasticity index values, the siltstone samples belong to class CIM, while the gray clay samples belong to class CIH. The consistency index values for siltstone are in the range of $I_c = 0.84\text{--}0.94$ and for gray clay from $I_c = 0.91\text{--}0.97$ (Figure 7). Based on the consistency index values, the samples are in a semi-hard consistency state.

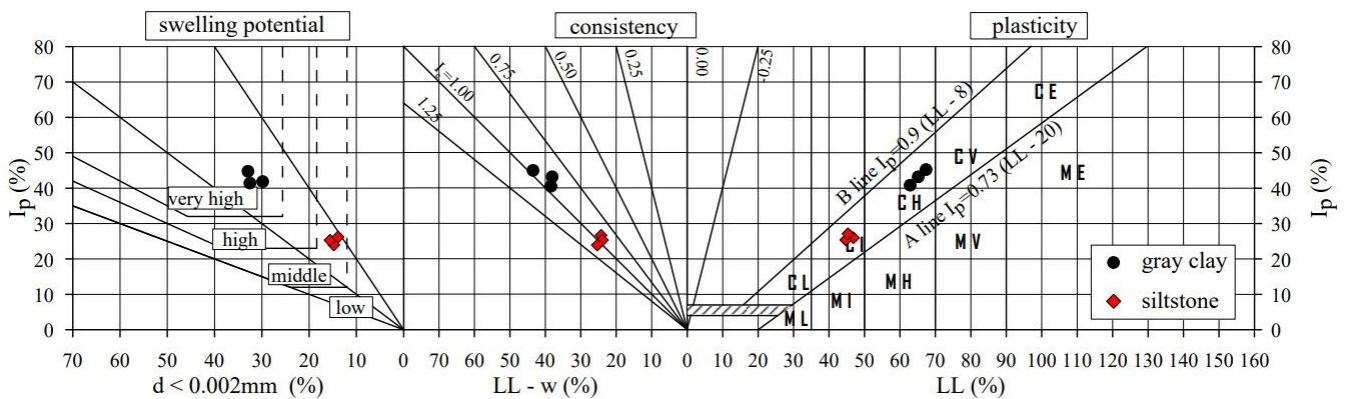


Figure 7. Identification and classification indicators of the tested samples.

The shear progression in the ring shear and direct shear apparatuses for the siltstone and clay samples is shown in Figures 8 and 9. Since these are remolded samples, they are dominated by unstable, hydrocolloidal bonds, making the activation of resistance smoother and more complex as it is accompanied by visible sample deformation, which is a result of the movement, even rotation, and shearing of elementary particles. Based on the low clay content and medium plasticity of the soil, combined with the specific shape of the stress–horizontal deformation curve, we can conclude that the movement mechanism is classified as transitional according to Lupini’s, 1981 [43]. Transitional soils are characterized by a

unique mixture of cohesive and non-cohesive properties. The low clay content suggests that, while the soil retains some cohesive characteristics, it may not exhibit the same level of plasticity as pure clay soils. The medium plasticity indicates that the soil has enough plastic behavior to deform under stress, but not excessively, which aligns with transitional behavior. Figure 8b illustrates a drastic drop in shear strength, which can be attributed to the higher content of clay fractions and the high plasticity of the soil. The platy clay minerals present in the soil exhibit a strong tendency to orient themselves parallel to the shear plane during deformation. This orientation contributes to a significant reduction in soil strength. According to Lupini's, this behavior is classified as a sliding mechanism. Skempton, 1970-1985 [2] concluded that, due to an increase in moisture, which results from the deformation and reorientation of clay particles parallel to the shear direction, there is a distinct drop in strength in overconsolidated clay after reaching the peak drained strength.

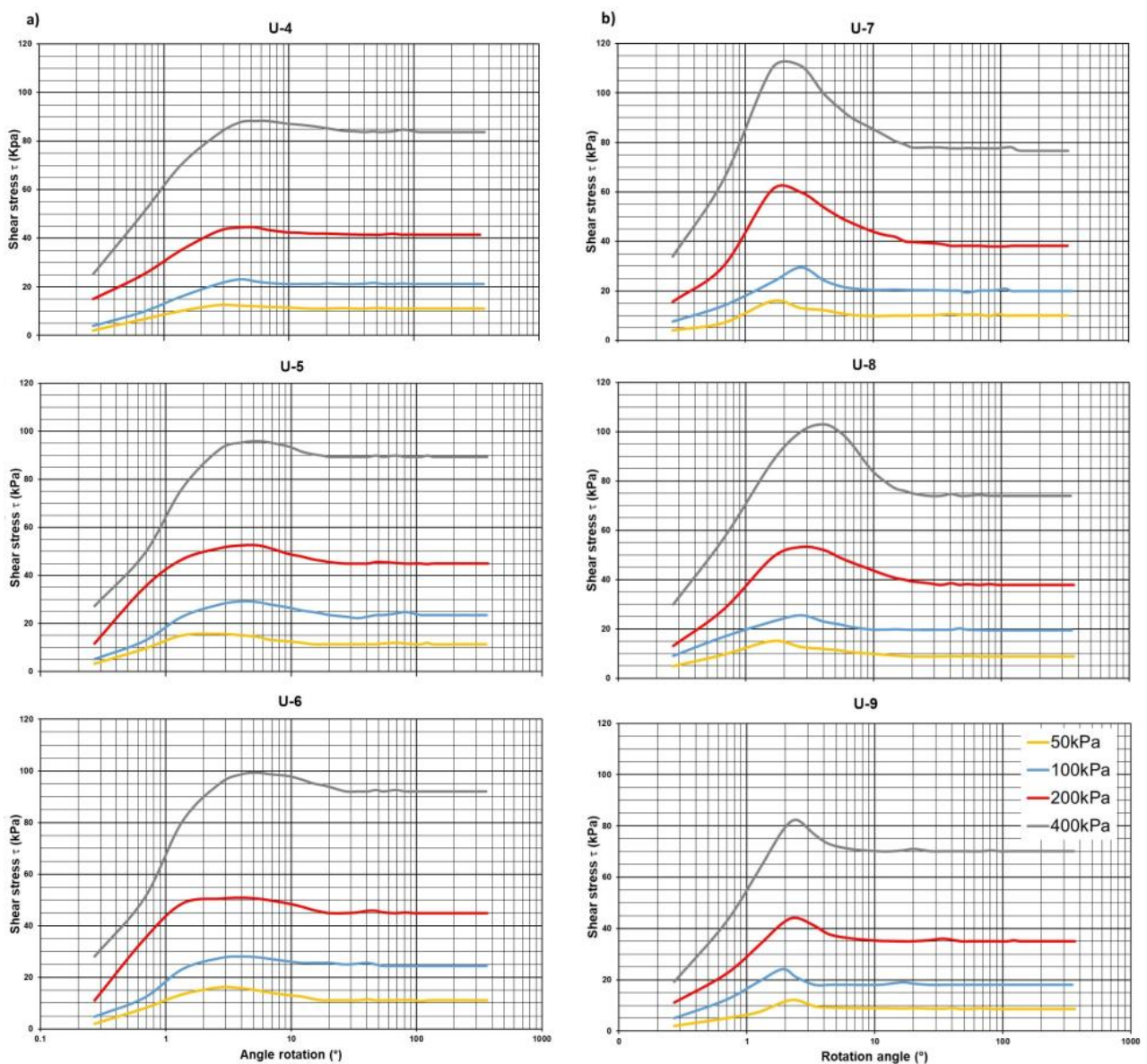


Figure 8. Shear stress versus rotation angle for (a) siltstone (b) gray clay.

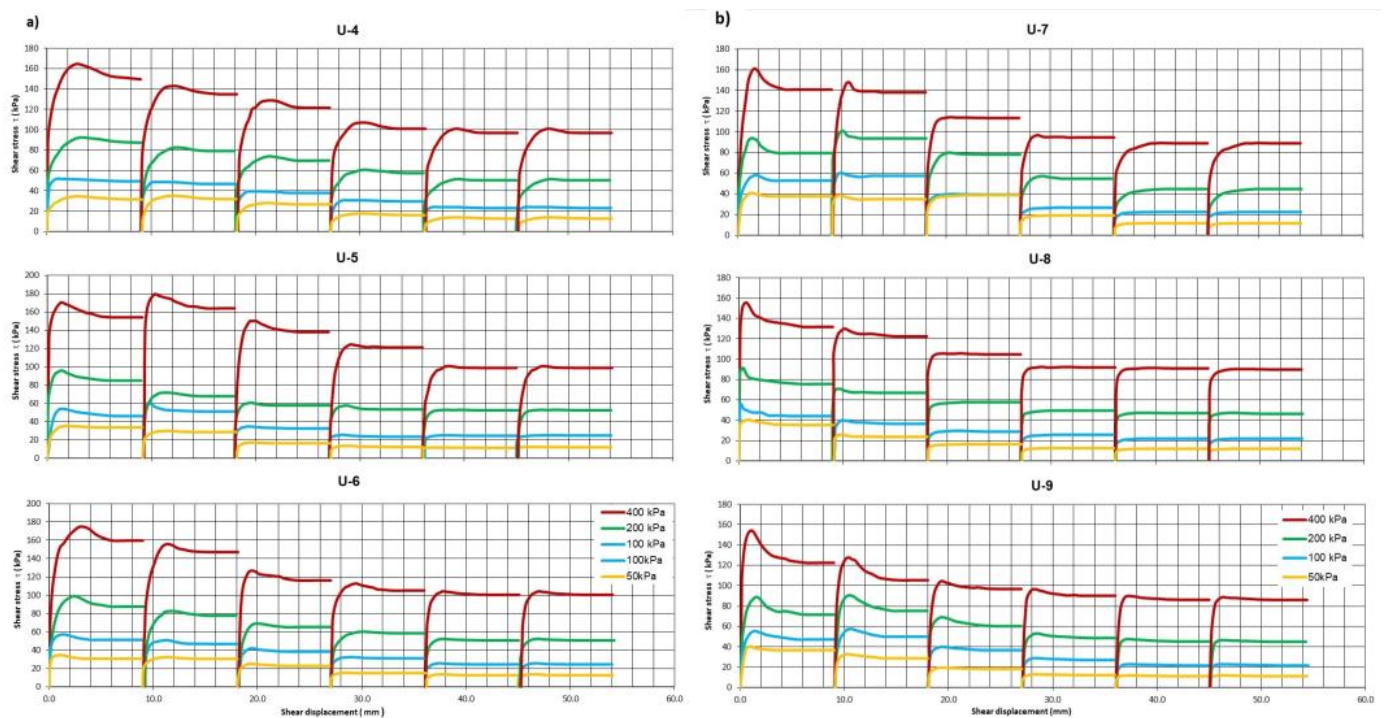


Figure 9. Shear stress versus horizontal displacement for (a) siltstone (b) gray clay.

In direct shear tests, after the first and second cycles and returning the shear box to its original position, due to the orientation of particles in the shear plane, samples U-5 (curve at normal stresses of 100 and 400 kPa), U-7 (curve at 100 kPa), and U-9 (curve at 100 and 200 kPa) exhibited accumulation and the “rabbit’s paw” effect, leading to a sudden increase in shear stress (Figure 9). The mechanism of material displacement in the form of accumulation and stretching (spreading) resembles a rabbit’s paw, and this phenomenon is colloquially referred to in Serbian as the “rabbit’s paw” effect. Shear stress–horizontal displacement curves in reverse DS tests can sometimes be very difficult to interpret due to renewed peaks with changes in shear direction and the shape of the shear stress–horizontal displacement curve [43].

Shear strength parameters are defined by cohesion and the angle of internal friction [44,45]. However, the residual angle of internal friction varies depending on the soil properties and the magnitude of the normal stress, assuming that the residual cohesion of the soil is zero [2,29,40,46]. After reaching the residual state, all internal adhesive and cohesive effects within the specimen are depleted. At this stage, the particles in the specimen have lost their ability to maintain a mutual connection, meaning that there are no longer any additional cohesive forces to bind them together and it is considered that the value of cohesion is equal to zero. The values of cohesion obtained from testing ranged up to 0.4 kPa, and considering the previously mentioned points, it was adopted for further consideration that cohesion is equal to zero.

The residual values of the angle of internal friction obtained in the DS apparatus for siltstone were in the range of $\phi'_R = 13.7\text{--}14.1^\circ$, while for gray clay they were $\phi'_R = 12.2\text{--}12.6^\circ$ (Figure 10).

The residual values of the angle of internal friction obtained with the RS apparatus for siltstone were in the range of $\phi'_R = 11.8\text{--}12.9^\circ$, while for gray clay, they were in the range of $\phi'_R = 9.9\text{--}10.8^\circ$ (Figure 10). As previously mentioned, a cohesion value of $c'_R = 0$ kPa was adopted for result interpretation.

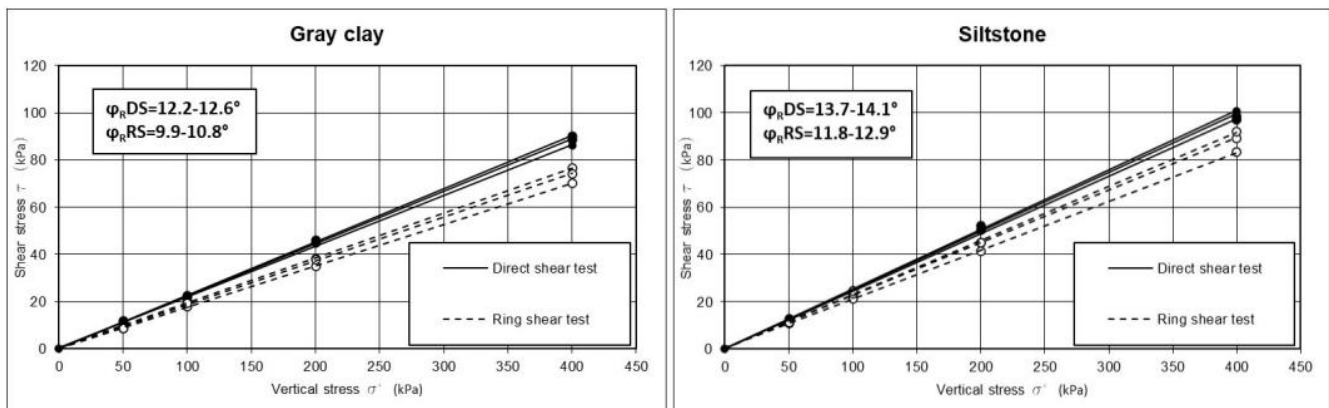


Figure 10. Values of the residual shear strength parameters depending on the testing method.

Generally speaking, based on the obtained results, it can be concluded that the residual angles of shear strength obtained from the RS for gray clay are 1.7–2.3° lower than the angle of internal friction obtained through the classical method for determining residual shear strength parameters in the DS apparatus. For siltstone samples, the difference in the residual angles of internal friction obtained from DS and RS was somewhat smaller, with values being 1.2–1.9° higher than those obtained from RS.

According to Vithana et al., 2011 [47], the results of direct shear tests on bentonite and mudstone samples are nearly twice those from ring shear tests, and for loess, siltstone, and alluvial loess samples, they range from around 1.02 to 1.3. Chen & Liu, 2013 [48], on the other hand, obtained similar ϕ'_R values using both apparatuses. Anaii et al., 1988 [49] found that modified tests on Bromhead’s ring shear apparatus yield lower values of residual friction angle compared to reverse direct shear tests. Rakić et al., 2011 [50] reported higher values in the DS apparatus compared to the RS apparatus for highly plastic carbonaceous clay and siltstone samples from the open-pit mine “Tamnava-West Field,” with higher values of 4–4.6° for clay and 1.3–2.0° for siltstone. Based on silt samples from a large landslide in Brazil, Heidemann, 2020 [51] reported internal friction angles of 12.0° in the DS apparatus and 7.7° in the RS apparatus. Fang, 2024 [52] reported ϕ'_R values of 32.94–13.97° for 15 artificially prepared samples taken from the embankments of a dam reservoir with varying amounts of fine particles ($d \leq 0.075$ mm) and concluded that the residual shear strength of soil decreases with an increase in the percentage of fine particles.

To determine the existence of a statistical difference between the values of the residual angle of internal friction obtained using the DS and RS apparatuses, as well as differences between the isolated geotechnical layers, the Tukey–Kramer test was conducted (Table 1). The results indicate a significant difference between the values of the angle of internal friction obtained from the DS and RS apparatuses. Additionally, the observed difference in the angle of internal friction values between the isolated geotechnical layers obtained using both apparatuses was confirmed by this analysis.

Table 1. Statistical differences of the residual angle of internal friction of the selected groups of samples.

Comparison	Absolute Difference	Critical Range	Result
ϕ_R DS vs. ϕ_R DS	1.5	0.441	Means significantly different
ϕ_R RS vs. ϕ_R RS	2.03	1.210	Means significantly different
ϕ_R RS vs. ϕ_R DS	1.77	1.560	Means significantly different

3.1. Site-Specific Correlation

To date, several correlations have been published between the parameters of residual shear strength and the physical parameters of soil (percentage of clay fractions and

plasticity index) across different soil types using various types of direct and ring shear apparatuses [29,40,43,45,52].

For a relatively small number of soil samples from the open pit mine Drmno (six samples), a correlation analysis was performed on the obtained values of residual angles of internal friction from the DS and RS apparatuses and the percentage of fractions $d < 0.002$ mm, as well as the plasticity index (I_p).

Figure 11 shows the correlation of the values of the residual angle of internal friction obtained from six soil samples in the DS and RS apparatuses.

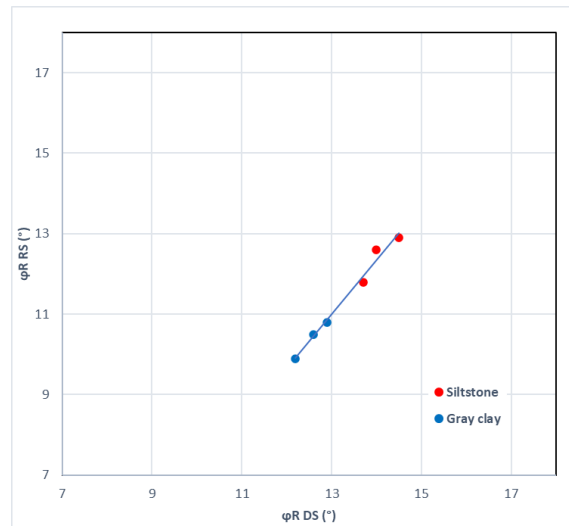


Figure 11. Correlation values of the residual angle of internal friction obtained from the DS and RS apparatuses.

The correlation between the angle values measured in the two shear apparatuses can be expressed by a linear relationship:

$$\varphi'_{R RS} = 1.347\varphi'_{R DS} + 6.5206 \tag{3}$$

where $\varphi'_{R RS}$ is the angle obtained in the RS apparatus, and $\varphi'_{R DS}$ is the angle value obtained from the DS apparatus.

A correlation has also been established between the plasticity index and the residual angles of internal friction obtained from the DS and RS apparatuses, as shown in Figure 12. The values of the coefficients of determination for the relationships between the parameters I_p - $\varphi'_{R RS}$ and I_p - $\varphi'_{R DS}$ are 0.91 and 0.92, respectively.

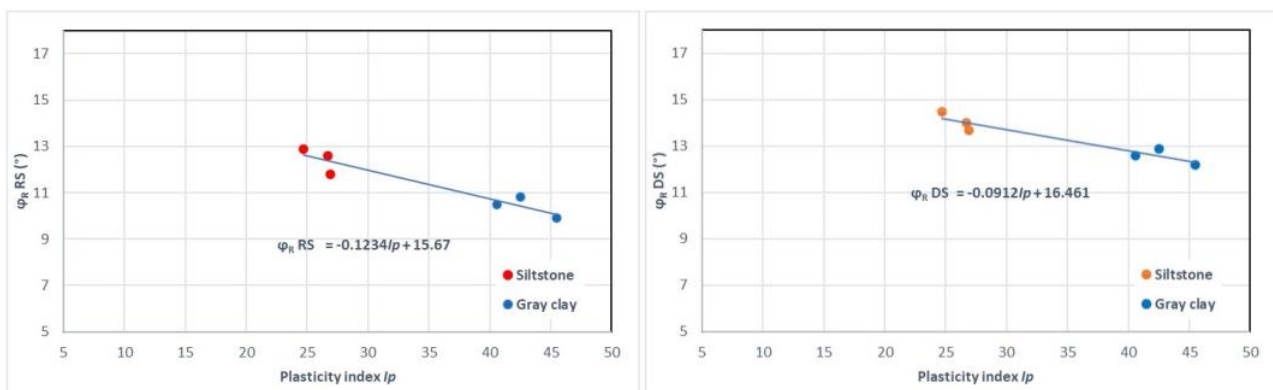


Figure 12. Correlation values between the plasticity index (I_p) and the residual angle of internal friction obtained from the DS (right) and RS (left) apparatuses.

Figure 13 shows the correlation between the values of the residual angle of internal friction and the clay fractions (less than 0.002 mm). The correlation between these values is expressed by a linear relationship, with the coefficients of determination for $d < 0.002 \text{ mm}-\varphi'_R$ RS and $d < 0.002 \text{ mm}-\varphi'_R$ DS being 0.86 and 0.88, respectively.

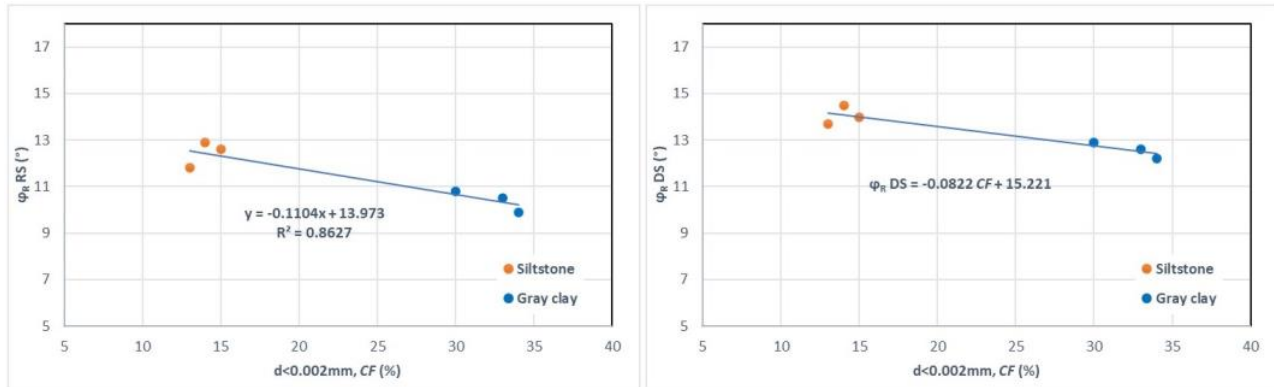


Figure 13. Correlation values between the percentage of fractions less than 0.002 mm and the residual angle of internal friction obtained from the DS (right) and RS (left) apparatuses.

All the presented correlations confirmed a negative correlation between the residual angle of internal friction and the physical parameters of the soil (Figures 12 and 13) and are useful for estimating trends at the studied location. However, they cannot be applied in a general sense in geotechnical practice. Collotta et al., 1989 [53] emphasized that similar correlations with a larger number of samples (from different locations) can yield more significant variability in the variables.

3.2. Practical Application of Research Results

Through the analysis of the residual strength parameters of soils in overburden sediments, it is possible to significantly contribute to the optimization of the slope angle of the final slope of surface mines. This practice is crucial in the design and dimensioning of operational and final slopes in surface mining. By considering the geomechanical characteristics of the sediments, mines can more effectively manage slope stability and reduce the risk of landslides.

Increasing the angle of the final slope, with a proper understanding and application of soil strength parameters, can lead to significant cost savings in mining operations and the opening of mines. Additionally, this approach can improve the overall efficiency of mining operations, allowing for greater production and a reduction in the resources needed to support slope stability.

Therefore, it is important to consider not only the current geological conditions when designing slopes but also the long-term stability and behavior of materials under changing working conditions.

4. Conclusions

In this study, the principles of performing ring and direct shear tests are described, and specific results obtained from siltstone and gray clay samples from the overburden of the third coal layer at the open pit mine Drmno are presented. Based on these results, a comparative analysis of the residual values was conducted. The general conclusions are as follows:

- The values of the residual angle of internal friction for gray clay obtained using the RS apparatus are 1.7–2.3° lower and for siltstone, 1.2–1.9° lower than those obtained using the DS apparatus;
- There is also a decrease in the residual angle of internal friction as the percentage of clay fractions in cohesive soils increases;

- The presented correlations between the residual angle of friction and the plasticity index and/or grain size composition cannot be generalized and only apply to the studied location;
- The proposed correlations should only be used when time and financial constraints do not allow for actual tests to determine residual shear strength, and they should only be considered as preliminary. However, in all other cases, conducting specific tests will provide a much more reliable assessment of the residual strength properties of the tested soil.

Author Contributions: Methodology, S.Ć.; software, S.Ć.; validation, S.Ć. and N.Ž.; formal analysis, S.Ć. and N.Ž.; investigation, S.Ć. and T.Đ.; data curation, S.Ć. and N.Ž.; writing—original draft preparation, S.Ć.; writing—review and editing, D.R. and N.Ž.; visualization, S.Ć.; supervision, N.Ž., D.R., and K.D. All authors have read and agreed to the published version of the manuscript.

Funding: This research was supported by the Ministry of Education, Science and Technological Development of the Republic of Serbia, Reg. No. 451-03-66/2024-03/200012 and Reg. No. 451-03-65/2024-03/2000169.

Institutional Review Board Statement: Not applicable.

Informed Consent Statement: Not applicable.

Data Availability Statement: The data are contained within the article. Additional data are available upon request from the corresponding author.

Acknowledgments: All the tests of residual shear strength were conducted at the Geomechanics Laboratory of the Mining Institute in Belgrade.

Conflicts of Interest: The authors declare no conflicts of interest.

References

1. Lambe, T.W.; Whitman, R.V. *Soil Mechanics*; John Wiley and sons, Inc.: Hoboken, NJ, USA, 1969; p. 559.
2. Skempton, A.W. Residual strength of clays in landslides, Folded Strata and the Laboratory. *Geotechnique* **1985**, *35*, 3–18. [[CrossRef](#)]
3. Bell, A.L. Lateral pressure and resistance of clay and the supporting power of clay foundations. *Min. Proc. Inst. Civ. Eng.* **1915**, *199*, 233–272.
4. Skempton, A.W. Arthur Langtry Bell (1874–1956) and his contribution to soil mechanics. *Géotechnique* **1958**, *8*, 143–157. [[CrossRef](#)]
5. Casagrande, A.; Albert, S.G. *Research on the Shearing Resistance of Soils*; MIT Report; MIT: Cambridge, MA, USA, 1932.
6. Matthews, M.C.; Clayton, C.R.I.; Own, Y. The use of field geophysical techniques to determine geotechnical stiffness parameters. *Geotech. Eng.* **2000**, *143*, 31–42. [[CrossRef](#)]
7. Babalola, Z. *Direct Shear and Direct Simple Shear Tests: A Comparative Study of the Strength Parameters and Their Dependence on Moisture and Fines Contents*; University of Cape Town: Cape Town, South Africa, 2016; p. 16.
8. Hvorslev, M.J. A ring shearing apparatus for the determination of the shearing resistance and plastic flow of soils. In Proceedings of the 1st International Conference on Soil Mechanics and Foundation Engineering, Boston, MA, USA, 22–26 June 1936; Volume 2, pp. 125–129.
9. Hvorslev, M.J. Torsion shear tests and their place in the determination of the shearing resistance of soils. *Proc. Am. Soc. Test. Mater.* **1939**, *39*, 999–1022.
10. La Gatta, D.P. *Residual Strength of Clay and Clay-Shales by Rotation Shear Tests*; Harvard Soil Mechanics Series; Harvard University Press: Cambridge, MA, USA, 1970; Volume 86.
11. Bishop, A.W.; Green, G.E.; Garga, V.K.; Andersen, A.; Brown, J.D. A new ring shear apparatus and its application to the measurement of residual strength. *Geotechnique* **1971**, *21*, 273–328. [[CrossRef](#)]
12. Bromhead, E.N. A simple ring shear apparatus. *Ground Eng.* **1979**, *12*, 40–44.
13. Savage, S.B.; Sayed, M. Stresses Developed by Dry Cohesionless Granular Materials Sheared in an Annular Shear Cell. *J. Fluid Mech.* **1984**, *142*, 391–430. [[CrossRef](#)]
14. Hungr, O.; Morgenstern, N.R. High Velocity Ring Shear Tests on Sand. *Geotechnique* **1984**, *34*, 415–421. [[CrossRef](#)]
15. Garga, V.K.; Sedano, J.A. Steady state strength of sands in a constant volume ring shear apparatus. *Geotech. Test. J.* **2002**, *25*, 414–421. [[CrossRef](#)]
16. Tika, T.E.; Hutchison, J.N. Ring shear tests on soil from the Viont landslide slip surface. *Geotechnique* **1999**, *49*, 59–74. [[CrossRef](#)]
17. Bromhead, E.N.; Curtis, R.D. A Comparison of Alternative Methods of Measuring the Residual Strength of London Clay. *Ground Eng.* **1983**, *16*, 39–41.
18. Sassa, K.; Fukuoka, H.; Wang, G.; Ishikawa, N. Undrained dynamic-loading ring-shear apparatus and its application to landslide dynamics. *Landslides* **2004**, *1*, 7–19. [[CrossRef](#)]

19. Cullen, R.M.; Donald, I.B. Residual strength determination in direct shear. In Proceedings of the 1st Australia—New Zealand Conference on Geomechanics, Melbourne, Australia, 9–13 August 1971; Volume 1, pp. 1–10.
20. Wen, B.P.; Aydin, A.; Duygoren-Aydin, N.S.; Li, Y.R.; Chen, H.Y.; Xiao, S.D. Residual strength of slip zones of large landslides in Three Gorges area, China. *Eng. Geol.* **2007**, *93*, 82–98. [[CrossRef](#)]
21. Casagli, N.; Dapporto, S.; Ibsen, M.L.; Tofani, V.; Vannocci, P. Analysis of the landslide triggering mechanism during the storm of 20th–21st November 2000, in Northern Tuscany. *Landslides* **2006**, *3*, 13–21. [[CrossRef](#)]
22. Okada, Y.; Ochiai, H.; Okamoto, T.; Sassa, K.; Fukuoka, H.; Igwe, O. A complex earth slide—Earth flow induction by the heavy rainfall in July 2006, Okaya City, Nakagano Prefecture, Japan. *Landslides* **2007**, *4*, 197–203. [[CrossRef](#)]
23. Van Asch, T.W.; Van Beek, L.P.H.; Bogaard, T.A. Problems in predicting the mobility of slow-moving landslides. *Eng. Geol.* **2007**, *91*, 46–55. [[CrossRef](#)]
24. *ASTM Standard D7608-10*; Standard Test Method for Torsional Ring Shear Test to Determine Drained Fully Softened Shear Strength and Nonlinear Strength Envelope of Cohesive Soils (Using Normally Consolidated Specimen) for Slopes with no Preexisting Shear Surfaces. ASTM International: West Conshohocken, PA, USA, 2010.
25. Wang, G.; Suemine, A.; Furuya, G.; Kaibori, M.; Sassa, K. Rainstorm-induced landslides at Kisawa village, Tokushima Prefecture, Japan, August 2004. *Landslides* **2005**, *2*, 235–242. [[CrossRef](#)]
26. Fukuoka, H.; Sassa, K.; Wang, G. Influence of shear speed and normal stress on the shear behavior and shear zone structure of granular materials in naturally drained ring shear tests. *Landslides* **2007**, *4*, 63–74. [[CrossRef](#)]
27. Li, Y.R.; Wen, B.P.; Aydin, N.S.; Lu, N.P. Ring shear tests on slip zone soils of three giant landslides in the Three Gorges, Project area. *Eng. Geol.* **2013**, *154*, 106–115. [[CrossRef](#)]
28. Hoyos, L.R.; Velosa, C.L.; Puppala, A.J. Residual shear strength of unsaturated soils via suction-controlled ring shear testing. *Eng. Geol.* **2014**, *172*, 1–12. [[CrossRef](#)]
29. Kimura, S.; Nakamura, S.; Vithana, S.B.; Sakai, K. Shearing rate effect on residual strength of landslide soils in the slow rate range. *Landslides* **2014**, *11*, 969–979. [[CrossRef](#)]
30. *EN 1997-1:2007*; Eurocode 7: Geotechnical Design—Part 2: Ground Investigation and Testing. CEN: Brussels, Belgium, 2007.
31. *SRPS EN ISO 17892-1:2015/A1:2023*; Geotechnical Investigation and Testing—Laboratory Testing of Soil—Part 1: Determination of Water Content—Amendment 1. Institut for standardization of Serbia: Belgrade, Serbia, 2023.
32. *SRPS EN ISO 17892-4:2017*; Geotechnical Investigation and Testing—Laboratory Testing of Soil—Part 4: Determination of Particle Size Distribution. Institut for standardization of Serbia: Belgrade, Serbia, 2017.
33. *SRPS EN ISO 17892-12:2018/A1:2022*; Geotechnical Investigation and Testing—Laboratory Testing of Soil—Part 12: Determination of Liquid and Plastic Limits—Amendment 1. Institut for standardization of Serbia: Belgrade, Serbia, 2022.
34. Karimpour, F.M.; Jamshidi, C.R.; Soheili, F. Shear strength characteristics of sand mixed with EPS beads using large direct shear apparatus. *Electron. J. Geotech. Eng.* **2015**, *20*, 2205–2220.
35. *ASTM Standard D6467-13*; Standard Test Method for Torsional Ring Shear Test to Determine Drained Residual Shear Strength of Cohesive Soils. Annual Book of Standards; ASTM International: West Conshohocken, PA, USA, 2013; Volume 4.
36. Hayden, C.P.; Purchase-Sanborn, K.; Dewoolkar, M. Comparison of site-specific and empirical correlations for drained residual shear strength. *Geotechnique* **2018**, *68*, 1099–1108. [[CrossRef](#)]
37. Kiernan, M.; Xuan, M.; Montgomery, J.; Anderson, J.B. Integrated Characterization and Analysis of a Slow-Moving Landslide Using Geotechnical and Geophysical Methods. *Geosciences* **2022**, *12*, 404. [[CrossRef](#)]
38. Ramiah, B.K.; Dayalu, N.K.; Purushothamaraj, P. Influence of chemicals on residual strength of silty clay. *Soils Found.* **1970**, *10*, 25–36. [[CrossRef](#)]
39. Japanese Geotechnical Society. *The Soil Testing Standards, Guidelines and Methods*; Japanese Geotechnical Society: Tokyo, Japan, 2010; ISBN 978-4-88644-084-6.
40. Skempton, A.W. Long-term stability of clay slopes. *Geotechnique* **1964**, *4*, 143–147. [[CrossRef](#)]
41. Bromhead, E.N. *The Stability of Slopes*; Blackie Academic & Professional: Glasgow, UK, 1992.
42. *ISO 14688-2:2017*; Geotechnical Investigation and Testing—Identification and Classification of Soil—Part 2: Principles for a Classification. ISO: Geneva, Switzerland, 2017.
43. Lupini, J.F.; Skinner, A.E.; Vaughan, P.R. The Drained Residual Strength of Cohesive Soils. *Geotechnique* **1981**, *31*, 181–213. [[CrossRef](#)]
44. Terzaghi, K.; Peck, R.B. *Soil Mechanics in Engineering Practice*; John Wiley and Sons: Hoboken, NJ, USA, 1951.
45. Stark, T.D.; Choi, H.; McCone, S. Drained shear strength parameters for analysis of landslides. *J. Geotech. Geoenviron. Eng.* **2005**, *131*, 575–588. [[CrossRef](#)]
46. Maksimović, M. On the residual shearing strength of clays. *Géotechnique* **1989**, *39*, 347–351. [[CrossRef](#)]
47. Vithana, S.B.; Nakamura, S.; Gibo, S.; Yoshinaga, A.; Kimura, S. Correlation of large displacement drained shear strength of landslide soils measured by direct shear and ring shear devices. *Landslides* **2012**, *9*, 305–314. [[CrossRef](#)]
48. Chen, X.P.; Liu, D. Residual strength of slip zone soils. *Landslides* **2013**, *11*, 305–314. [[CrossRef](#)]
49. Anaii, J.T.; Boyce, J.R.; Rodgers, C.D. Comparison of alternative methods of measuring the residual strength of a clay. In *Transportation Research Record*; Transportation Research Board (TRB): Washington, DC, USA, 1988; Volume 1192, pp. 16–26.
50. Rakić, D.; Čaki, L.; Čorić, S.; Ljubojev, M. Residual strength parameters of high plasticity clays and alewives from open/pit mine “Tamnava—West field”. *Min. Eng.* **2011**, *1*, 39–48.

51. Heidemann, M.; Bressani, L.A.; Flores, J.A. Residual Shear Strength of a Residual Soil of Granulite. *Soil Rocks* **2020**, *43*, 31–41. [[CrossRef](#)]
52. Fang, C.; Li, Y.; Gu, C.; Xing, B. Effect of Fine-Grained Particles and Sensitivity Analysis of Physical Indexes on Residual Strength of Granite Residual Soils. *Coatings* **2024**, *14*, 105. [[CrossRef](#)]
53. Collotta, T.; Cantoni, R.; Pavesi, U.; Ruberl, E.; Moretti, P.C. A correlation between residual friction angle, gradation and the index properties of cohesive soils. *Géotechnique* **1989**, *39*, 343–346. [[CrossRef](#)]

Disclaimer/Publisher’s Note: The statements, opinions and data contained in all publications are solely those of the individual author(s) and contributor(s) and not of MDPI and/or the editor(s). MDPI and/or the editor(s) disclaim responsibility for any injury to people or property resulting from any ideas, methods, instructions or products referred to in the content.